Development and Statistical Optimization of Solid Lipid Nanoparticle Formulations of Fluticasone Propionate

Flutikazon Propiyonatının Katı Lipid Nanopartikül Formülasyonlarının Geliştirilmesi ve İstatistiksel Optimizasyonu

Gulin Amasya, CEYDA TUBA SENGEL-TURK, Ulya Badıllı, Nilüfer Tarımcı
Department Of Pharmaceutical Technology, Ankara University Faculty Of Pharmacy, 06100 Tandogan, Ankara/Turkey

Abstract

INTRODUCTION: The aim of this study was to develop Fluticasone propionate (FP)-loaded solid lipid nanoparticle (SLN) formulations using the factorial design approach.
METHODS: Tristearin percentages (X1) (1%, 2% and 4%) and homogenization cycles (X2) (2, 4, 8 cycles) were selected as independent variables in the factorial design. SLN formulations were optimized by multiple regression analysis (MLR) to evaluate the influence of the selected process and formulation independent variables on SLNs characteristics namely as encapsulation efficiency (Q1) and particle size (Q2). Polydispersity index and surface charge of the SLNs were also evaluated in this research. Besides, transmission electron microscopy, Differential scanning calorimetry and in vitro drug relase studies were carried out on the optimum SLN formulation.
RESULTS: MLR analysis indicated that as homogenization cycle (X2) increased in the production process, the mean particle size was decreased.
DISCUSSION AND CONCLUSION: This research displayed that FP-encapsulated SLNs with desired characteristics can be produced by varied the production and content variables of the formulations.

Keywords: Experimental Design, Fluticasone Propionate, Nanoparticles,

Özet

GİRİŞ ve AMAÇ: Bu çalışmanın amacı, faktöriyel tasarım yaklaşımını kullanarak Flutikazon propiyonat (FP) yüklü katı lipid nanopartikül formülasyonları geliştirmektir.
YÖNTEM ve GEREÇLER: Bu amaçla faktöriyel tasarımda Tristearin yüzdeleri (X1) (% 1, % 2 ve % 4) ve homojenizasyon döngüleri (X2) (2, 4 ve 8 döngü) bağımsız değişkenler olarak seçilmiştir. Seçilen işlem ve formülasyona ait bağımsız değişkenlerin, katı lipid nanopartikül formülasyonların enkapsülasyon etkinliği (Q1) ve partikül boyututları (Q2) üzerindeki etkisini değerlendirmek için çoklu regresyon analizi (MLR) ile optimize edilmiştir. Çalışmada ayrıca nanopartiküllere ait polidispersite indeksi ve yüzey yükleri de değerlendirilmiştir. Bunun yanı sıra optimum katı lipid nanopartikül formülasyonu üzerinde geçirimli elektron mikroskopu, difransiyel taramalı kalorimetre analizi ve in vitro etkin madde salım çalışmaları da yapılmıştır.
BULGULAR: MLR analizi, üretim sürecinde homojenizasyon döngüsü (X2) arttıkça, ortalama partikül boyutunun azaldığını göstermiştir.
TARTIŞMA ve SONUÇ: Bu araştırma, istenen özelliklere sahip FP yüklenmiş katı lipid nanopartiküllerin, formülasyonların üretim ve içerik değişkenlerini değiştirerek üretilebileceğini göstermektedir.

Anahtar Kelimeler: Deneysel tasarım, Flutikazon propionat, Nanopartiküller

INTRODUCTION

Topical corticosteroids are the most commonly used drugs in the practice of dermatology especially for the treatment of inflammatory skin diseases. However, their long-term application is restricted due to their local and systemic adverse effects. Several researches have been performed to enhance the anti-inflammatory efficiency of these active substances and to reduce their side effects[1-3].

Fluticasone propionate (FP) is a synthetic trifluorinated topical corticosteroid and has been classified as a potent anti-inflammatory, immunosuppressive and antiproliferative drug for the therapy of skin disorders such as atopic dermatitis and psoriasis[4,5]. It is a highly lipophilic substance and is characterized by high glucocorticoid receptor binding and activation[2]. FP is available in 0.005% ointment and 0.05% cream formulations for the treatment of the inflammatory skin disorders which are responsive to corticosteroids[5,6].

Dermal drug delivery means that the targeting of drugs to the different layers of skin with minimum systemic absorption. The accumulation of the drug in skin is an important issue for the therapy of the diseases such as atopic dermatitis, psoriasis, skin cancer etc[7,8]. In other words, drugs should reach the skin layers at an appropriate concentration and stay there for a certain time of period. However, the barrier function of the stratum corneum, which is the uppermost layer of epidermis, considerably restricts the penetration of drugs into skin[9]. Nanosized drug delivery systems receive a great deal of interest for dermal application since they offer several advantages. These advantages can be summarized as enhancing the skin penetration and reducing the side effects of active substances, achieving the site-specific drug targeting into skin, providing the sustained and/or controlled release of drugs and increasing the chemical stability of molecules[9-11]. Dermal drug delivery by liposomes[12]; niosomes[13]; nanoemulsions[14]; polymeric nanoparticles[15] and lipid nanoparticles[16-18] has been extensively researched by several groups.

Solid lipid nanoparticles (SLNs) were presented in the early 1990s with intent to extinguish the drawbacks of pre-existing colloidal drug delivery systems such as nanoemulsions, liposomes and polymeric nanoparticles[19, 20]. SLNs are produced by physiologically tolerated lipids or the mixture of lipids which are in solid state at body

and room temperature. SLNs have several advantages like biocompatibility, protection of drugs against degradation, modification of drug release rate and possibility of the large scale production without using organic solvents. Moreover, the structural similarity and interactions between the epidermal lipids and the lipid matrix of SLNs could enhance the skin permeation of the encapsulated drugs. The nanosize, narrow size distribution and the greater surface area of SLNs also facilitate the drug penetration into skin[21-23]. The controlled drug release can be achieved by using solid lipids because the mobility of drug is significantly lower in solid lipid matrix than in an oil droplet. Several types of solid lipids including fatty acids, triglycerides, partial glycerides, waxes and steroids can be used as the main ingredients of SLNs. The most frequently used surfactants are poloxamers, polysorbates, lecithins, polyvinyl alcohol and bile salts for providing the stabilization of nanodispersion[24-25].

There are various methods for production of SLNs as high pressure homogenization, microemulsion, high shear homogenization and/or ultrasonication, solvent emulsification-evaporation, solvent emulsification-diffusion, electrospraying, solvent injection, membrane contactor and supercritical fluid (SFC). High pressure homogenization is the most preferred method for manufacturing SLN dispersions since it exhibits several advantages compared to other techniques such as suitability for large scale industrial production, possibility of production without using an organic solvent and the quite short production time[26-27].

Factorial design is a statistical approach and conducts systematic scientific researches to determine the impact of the independent variables on the responses of the dependent variables. The main objective in the factorial design approach is to obtain the maximum information between the minimum sample size and the cause-effect relationship for optimization of the formulation[28]. For this purpose, factorial design approach makes controlled changes in input variables. The factorial design helps to scale the replies of the dependent variables based on the defined goals. Response surface methodology is also performed by applying factorial design[29,30]. The present investigation was aimed to develop FP-loaded SLNs using the factorial design approach. Optimization of various physico-chemical characteristics of SLNs was carried out using the 3^2 factorial design through Design Expert 6.0.8 software. Two formulation parameters, tristearin percentages (1%, 2% and 4%) and homogenization

cycles (2, 4, 8 cycles) were selected as independent variables. The response variables investigated to characterize the particles were the encapsulation efficiency percentage (*Q*1) and particle size (*Q*2) of the SLNs.

MATERIALS AND METHODS

Materials

FP was kindly supplied as a gift from Deva Drug Company (Istanbul, Turkey). Tristearin was obtained from Sigma Aldrich (USA). Tween 80 was purchased from Fluka (USA). All other reagents and chemicals were of analytical reagent grade.

Analytical Validation of the HPLC Method

The analytical validation of the HPLC method for the determination of FP was performed. The linearity, accuracy, precision, limit of detection and limit of quantification (LOD and LOQ) values of the HPLC method were calculated.

Optimization by 3^2 Factorial Design

Multiple linear regression (MLR) analysis was performed to investigate the factors affecting the final properties of SLNs31. Nine SLN formulations were prepared as per 32 factorial design to determine the impact of two independent variables; tristearin percentages (X1) and homogenization cycle (X2) on the two responses; entrapment efficiency percentage (Q1), and mean particle size (Q2) of the FP-loaded SLNs. Three levels (-1, 0 and 1) were designated for the testing of each factor. The regression equation of the fitted model for the responses was calculated using Eq.1.

$$Q = bo+b1X1+b2X2+b3X12+b4X22+b5X1X2 \quad \text{(Eq.1.)}$$

To evaluate the response variables in terms of interactive and polynomial terms, a statistical model was employed. In the model, *Q* is the independent variable; bo is the arithmetic average response of nine experiments, and b1, b2, b3, b4 and b5 are the forecasted co-efficient for the factor *X1* and *X2.* When two factors are changed at the same time, the term that indicates how the response changes are the interaction term (*X1X2*). Non-linearity is investigated through the polynomial terms (*X12* and *X22*). The results from factorial design were examined statistically using analysis of variance

(ANOVA) (4). The values and the levels of factors investigated in this research and the variable levels are displayed in Table 1.

Table 1. Actual values and variable leves designed through 3^2 factorial design of FP-loaded SLNs.

Preparation of SLN Formulations

FP loaded SLN formulations were prepared by high pressure homogenization technique. Tristearin was melted at a temperature which is 10°C above its melting point and 50 mg of FP was added into the melted lipid. Aqueous Tween 80 (1%) solution was also heated to the same temperature. Lipid phase and aqueous phase were mixed to obtain a pre-emulsion by Ultraturrax T25 (IKA, Germany) at 13500 rpm for 3 minutes. The hot pre-emulsion was subsequently homogenized by a high pressure homogenizer (Microfluidics M110L, USA) at a pressure of 1000 bar. Three different tristearin percentages (1%, 2% and 4%) and three different cycle numbers (2, 4, 8 cycles) were investigated based on two responses: encapsulation efficiency (*Q*1) and particle size (*Q*2). SLN dispersions were centrifuged using Vivaspin (MWCO=10000) at 4500 rpm for 30 minutes (Sigma 3K30, Germany) and then lyophilized.

Particle Size and Zeta Potential Analysis

The mean particle size and polydispersity index of FP loaded SLNs were determined using a dynamic light scattering analyzer (Nano ZS, Malvern, UK). The zeta potential values were determined from the electrophoretic mobility (Zetasizer Nano ZS, Malvern, UK). Before analysis, all samples were diluted 1000 times with ultrapure water.

Determination of Encapsulation Efficiency

For the determination of the encapsulation efficiency of SLN formulations, 10 mg of SLN was dissolved in methanol at 75°C. The solution was stirred using a magnetic stirrer in a tightly sealed vial. After that, the solution was ultrasonicated with 50% power for 5 minutes (Bandelin Sonoplus HD 2070, Germany) and then cooled to room temperature. It was centrifuged at 26000 rpm for 20 minutes at 4°C (Sigma 3K30, Germany) and then the supernatant was filtered from 0.22 µm cellulose acetate

membrane filter. The amount of FP was determined using an HPLC system (Agilent 1260 Infinity). Separation was carried out using NovaPak® C18 column (4 µm, 150 x 3.9 mm) (Waters, Ireland). The column temperature was set at 35ºC. The mobile phase composition was acetonitrile:water (60:40 v/v) and the flow rate was 1 ml/min. 10 µl of each sample was injected into the system and the samples were analyzed at a wavelength of 236 nm.

In vitro drug release study

The dialysis bag method was used in order to determine the in vitro release profile of FP from SLN formulation. SLN formulation corresponding to 5 mg of FP was placed into the hydrated dialysis membranes (MWCO = 12-14 kDa, Spectrapor-2). The mixture of 100 ml of PBS (phosphate buffered saline) pH 7.4:ethanol (70:30) was used as dissolution medium at 37^0C and under constant stirring (100 rpm). The samples were taken at specific time intervals during 24 hour. The medium was completely removed and replaced with 100 ml of fresh dissolution medium for each time point to provide a sink condition. Samples taken were filtered through 0.45 µm regenerated cellulose membrane filters and the amount of FP was determined by HPLC.

Transmission Electron Microscopy (TEM) Analysis

The morphological characterization of the FP-loaded SLNs was performed using FEI Tecnai Spirit transmission electron microscope (Osaka, Japan). Lipid nanoparticles were diluted with ultrapure water and then dispersion was placed on a copper grid. The sample was imaged at an accelerated voltage of 120 kV.

Differential Scanning Calorimetry (DSC) Analysis

Thermal analysis and crystallinity of pure FP, bulk lipid and FP-loaded SLNs were carried out by a differential scanning calorimeter (Shimadzu DSC-60, Japan). Five mg of sample was placed in hermetically sealed aluminum pans and heated from 20°C to 300°C at a rate of 5°C/min. Inndium used as a reference for calibration.

RESULTS AND DISCUSSION

Analytical Validation of the HPLC Method

Linearity

Each of the eight different concentration of FP was analyzed by HPLC for six times. The average peak areas were plotted vs concentrations and a linear relationship between peak area and concentration was observed. Excellent linearity was obtained between concentrations of 0.25 and 10 µg/ml in methanol with $r^2 = 0.9996$.

Accuracy

Solutions of FP in methanol at concentrations of 0.5 µg/ml, 4 µg/ml and 10 µg/ml were injected 6 times as a test sample. The concentrations of FP were calculated using the detector responses. The accuracy was determined in terms of the variation coefficient (relative standard deviation - RSD) of the percent recovery values. Since the RSD values obtained were less than or around 2%, the method was assumed to be accurate (Table 2).

Precision

The repeatability (intra-day precision) and intermediate (inter-day) precision of the method were evaluated. The repeatability of the method was determined by the analysis of 6 replicate injections of FP-methanol solutions and was expressed as the RSD of measured concentrations. As seen in Table 2, the RSD values were less than 2%. The intermediate precision of the HPLC method was defined by the RSD value of 12 injections performed on two different days and the RSD values were found to be less than 2% (Table 2). On the other hand, there is no statistically significant difference between the means of the measured concentrations obtained on two different days for each FP solution (p□0.05).

LOD and LOQ values

The LOD and LOQ values were calculated with respect to the following equations using the standard deviation (s) of the response and the slope (m) of the calibration curve. While LOD value was found to be 0.09 µg/ml, LOQ value was 0.28 µg/ml.

LOD = 3.3 x s / m

LOQ = 10 x s / m

Table 2. The RSD% values obtained for the analytical validation parameters

Formulation Optimization by 3^2 Factorial Design

Tristearin percentages were varied from 1%, 2%, and 4%. These three different ratios were tested at three different homogenization cycle of 2, 4 and 8. In this way, nine formulations were prepared as per 3^2 factorial design. The magnitude and sign of the main influence indicate the relative effect of each factor on the response by means of polynomial equations. Table 3 gives the predicted and the observed values of responses (*Q1*, *Q2*). The predicted values were derived from the equations and the observed values were determined from experimental results.

Table 3. Observed and predicted responses of FP-loaded SLNs.

Table 4 shows the results of model co-efficients estimated by MLR and the ANOVA of the investigated model for all responses. The quality of the model developed was evaluated based on the regression coefficient values. The determination co-efficient (r^2 value) for the response *Q2* was nearer to 1 indicating that there was a good agreement between the observed and the predicted measures from the model. The Negative sign in front of the co-efficients is indicated that the response of the nanoparticles increases when the independent factor was decreased, and the positive sign for the co-efficients showed the positive effect of the independent factors on the observed replies. The Model F-value of 3.87 for *Q1* response implied there was a 5.30% probability that a "Model F-Value" of this magnitude could be caused by noise. On the other hand, the Model F-value of 57.71 for *Q2* response indicated that the model was statistically meaningful. The possibility of such a large "Model F-Value" due to noise is only 0.01%[28,31,32].

Table 4. Results of model co-efficients estimated by MLR and the ANOVA of the fitted model for all responses.

Figure 1 shows the linearity plots between the *Q*1 and *Q*2 values. The correlation graphs that show linearity between actual and predicted response variables indicated that the fit to the model was at an excellent level for *Q*2 ($p<0.05$) whereas the linear correlation plots showed a low compliance to the model for *Q*1 ($p>0.05$) (Figure 1). This situation is also evidenced by the calculated F value for *Q*1 model. The F value of the *Q*1 model (F=3.87) is smaller than the tabulated F value (Ftab=4.46), indicating that the model is not statistically significant (Figure 1, and also the P values in Table 4).

Figure 1. Linearity correlation graphs between actual and predicted values of (A) *Q*1, (B) *Q*2.

As seen from Table 3, drug entrapment efficiency of all factorial formulations was produced with a broad range of 27.07-94.65%. Drug entrapment efficiency was not affected significantly by both the level of *X1* and *X2* ($p>0.05$). Generally, as seen in P values that indicated the significance of the co-efficients (Table 4), both of the independent factors - *X*1 and *X*2 - had not a strong effect on the drug entrapment efficiency (*Q1*) ($p>0.05$).

When the average particle size of the SLNs was investigated depending on the variation of homogenization cycle (*X*2) at each tristearin percentages (*X*1), it was observed that as *X*2 increased from 2 to 8, the mean particle size decreased significantly ($p<0.05$). The average particle size of SLNs ranged from 130.9±3.30 to 352.9±10.93 nm. Generally, from the P values of the co-efficients that presented in Table 4, it was concluded that both of the investigated variables - *X*1 and *X*2 - had a major influence on the response *Q*2 ($p<0.05$). The biggest mean particle size was observed in the lowest level of *X*1 (1%) and the lowest level of *X*2 (2 cycle) in factorial formulation SLN1.

PDI, which is the indicator of homogeneity of particle size distribution in nano-sized drug delivery systems, is generally expressed as smaller than 0.3 for narrow size distribution[28,32]. PDI values of the all factorial formulations were found between 0.181

and 0.497 (Figure 2). It was observed that the factorial formulations which contain tristearin with a percentage of 1 or 2, showed a wide size distribution (PDI>0.2) based on the homogenization cycles investigated except at the formulations that contained percentage of tristearin of 2% at homogenization cycle of 8 (SLN6 coded formulation). As tristearin percentage increased from 1% or 2% to 4%, the PDI values were found less than 0.3 indicating a uniform size distribution.

Figure 2. PDI values of the FP-loaded SLN formulations.

Surface charge of the nano-sized particles is the potential at the hydrodynamic shear plane and informs about the particle stability in dispersion[31]. All of the SLNs exhibited negative surface charge between -19.5 and -29.7 mV. The surface charge of SLNs was not affected significantly from both the variation of tristearin percentages and homogenization cycle (Figure 3).

Figure 3. Surface charge of the FP-encapsulated SLN formulations.

Simplified models were also utilized to draw contour plots for analyzing the influence of independent variables. The contour plots give a diagrammatical demonstration of the values of the response. As shown in the contour plot of *Q*2 (Figure 4B), the linear existence of the plot was an indication of the linear relationship between *X*1 and *X*2 independent variables whereas the contour plots that belonged to *Q*1 (Figure 4A), was found to be non-linear, demonstrating a nonlinear relationship between *X*1 and *X*2.

Figure 4. Contour plots of FP-loaded SLNs showing the influence of *X*1 and *X*2 on (A) *Q*1, (B) *Q*2.

According to the in vitro release profile study of FP loaded SLN as shown in Figure 5; prolonged release was obtained without any initial burst effect. The nature of the lipid matrix affects the release profile of the active substance. It is thought that FP loaded SLN formed in a core-shell model with a drug-enriched core. This may be responsible for the slow release.

Figure 5. In vitro drug release profile of FP loaded SLN

TEM micrographs of FP loaded SLN are shown in Figure 6. TEM analysis confirmed the spherical shape and colloidal sizes of the FP loaded SLN.

Figure 6. TEM micrograph of the optimal formulation

Differential Scanning Calorimetry (DSC) Analysis

When the DSC thermograms given in Figure 7 were examined, it was observed that pure FP is decomposed by a small exothermic peak at 271.72°C. This result is in agreement with a previous study by El-Gendy et al. and also Dai et al. [33,34].The peak of the active agent thus observed also indicated that the FP was a crystal structure. When the DSC thermogram of pure form of Tristearin was evaluated, it was seen that Tristearin produced a small exothermic shoulder peak at 49.89°C at first and then it gave a large endothermic peak at 60.73°C, which indicated the presence of a crystal structure of the Tristearin[35]. When the DSC thermogram of the optimum formulation was examined, it was detected that the exothermic peak of FP disappeared. This situation was interpreted as the crystal structure of FP was returned to amorphous nature within the SLN matrix structure. When the thermogram of the optimum formulation was examined for Tristearin peaks, it was seen that the exothermic shoulder peak of Tristearin disappeared where the main endothermic main peak at

57.02°C remained the same shape with the same sharpness. This situation was interpreted as the fact that Tristearin in the SLN formulation preserved a large proportion of its crystal structure.

Figure 7. DSC thermograms of pure FP, Tristearin and optimum formulation.

CONCLUSIONS

FP-loaded SLNs were successfully fabricated using high pressure homogenization method. 32 experimental design and a contour plot analysis were performed by using a computer based program to set up the best formulation conditions with a limited number of experiments. This study showed that tristearin percentages and the homogenization cycles used in the SLN formulations were affected significantly the physico-chemical characteristics of FP-loaded SLNs. According to a factorial design study obtained in this research, the optimum formulation could be achieved with the content of 4% tristearin and the homogenization cycle 4.

REFERENCES

1. Brazzini B, Pimpinelli N. New and established topical corticosteroids in dermatology: clinical pharmacology and therapeutic use. Am J Clin Dermatol, 2002; 3(1): 47-58.
2. Roeder A, Schaller M, Schafer-Korting M, Korting HC. Safety and efficacy of fluticasone propionate in the topical treatment of skin diseaes. Skin Pharmacology and Physiology. 2005; 18: 3-11.
3. Gual A, Pau-Charles I, Abeck D. Topical corticosteroids in dermatology: from chemical development to galenic innovation and therapeutic trends. J Clin Exp Dermatol Res. 2015; 6(2): 1-5.
4. Doktorovová S, Araújo J, Garcia ML, Rakovsky E, Souto EB. Formulating fluticasone propionate in novel PEG-containing nanostructured lipid carriers (PEG-NLC). Colloids and Surfaces B: Biointerfaces. 2010; 75: 538–542.

5. Korting HC, Schöllmann C. Topical fluticasone propionate: intervention and maintenance treatment options of atopic dermatitis based on a high therapeutic index. JEADV. 2012; 26, 133–140.
6. Spencer CM, Wiseman LR. Topical fluticasone propionate: a review of its pharmacological properties and therapeutic use in the treatment of dermatological disorders. BioDrugs. 1997; 7(4): 318-334.
7. Brown MB, Martin GP, Jones SA, Akomeah FK. Dermal and transdermal drug delivery systems: current and future prospects. Drug Deliv. 2006; 13: 175-187.
8. Badilli U, Gumustas M, Uslu B, Ozkan SA. Lipid Based Nanoparticles for Dermal Drug Delivery, In: Grumezescu AM, Andrew W, eds. Organic Materials as Smart Nanocarriers for Drug Delivery; Applied Science Publishers-Elsevier; 2018; 9: 369-413.
9. Gupta M, Agrawal U, Vyas SP. Nanocarrier-based topical drug delivery for the treatment of skin diseases. Expert Opin Drug Deliv. 2012; 9(7): 783-804.
10. Papakostas D, Rancan F, Sterry W, Blume-Peytavi U, Vogt A. Nanoparticles in dermatology. Arch Dermatol Res. 2011; 303: 533-550.
11. Zhang Z, Tsai PC, Ramezanli T, Michniak-Kohn, BB. Polymeric nanoparticles-based topical delivery systems for the treatment of dermatological diseases. WIREs Nanomed Nanobiotechnol. 2013; 5: 205–218.
12. Lopez-Pinto JM, Gonzalez-Rodriguez ML, Rabasco AM. Effect of cholesterol and ethanol on dermal delivery from DPPC liposomes. International Journal of Pharmaceutics. 2005; 298: 1–12.
13. Manconi M, Sinico C, Valenti D, Lai F, Fadda AM. Niosomes as carriers for tretinoin III. A study into the in vitro cutaneous delivery of vesicle incorporated tretinoin. Int J Pharm. 2006; 311: 11-19.
14. Shakeel F, Haq N, Al-Dhfyan A, Alanazi FK, Alsarra IA. Double w/o/w nanoemulsion of 5-fluorouracil for self-nanoemulsifying drug delivery system. Journal of Molecular Liquids. 2014; 200:183–190.
15. Alvarez-Roman R, Naika A, Kaliaa YN, Guya RH, Fessia H. Skin penetration and distribution of polymeric nanoparticles. Journal of Controlled Release. 2004; 99: 53-62.
16. Souto EB, Wissing SA, Barbosa CM, Müller RH. Development of a controlled release formulation based on SLN and NLC for topical clotrimazole delivery, Int J Pharm. 2004; 278: 71–77.

17. Gainza G, Pastor M, Aguirre JJ, Villullas S, Pedraz JL, Hernandez RM, Igartua M. A novel strategy for the treatment of chronic wounds based on the topical administration of rhEGF-loaded lipid nanoparticles: in vitro bioactivity and in vivo effectiveness in healing-impaired db/db mice. Journal of Controlled Release. 2014; 185: 51–61.
18. Pradhan M, Singh D, Murthy SN, Singh MR. Design, characterization and skin permeating potential of fluocinolone acetonide loaded nanostructured lipid carriers for topical treatment of psoriasis. Steroids. 2015; 101: 56–63.
19. Gasco MR. Method for producing solid lipid microspheres having a narrow size distribution. US Patent. 1993; 5: 250-236.
20. Müller RH, Radtke M, Wissing SA. Solid lipid nanoparticles (SLN) and nanostructured lipid carriers (NLC) in cosmetic and dermatological preparations. Advanced Drug Delivery Reviews. 2002; 1:131-155.
21. Zhai Y, Zhai G. Advances in lipid based colloid systems as drug carrier for topic delivery. Journal of Controlled Release. 2014; 193: 90-99.
22. Sala M, Diab R, Elaissari A, Fessi H. Lipid nanocarriers as skin drug delivery systems: Properties, mechanisms of skin interactions and medical applications. International Journal of Pharmaceutics. 2018; 535: 1–17.
23. Garcês A, Amaral MH, Sousa Lobo JM, Silva AC. Formulations based on solid lipid nanoparticles (SLN) and nanostructured lipid carriers (NLC) for cutaneous use: A review. European Journal of Pharmaceutical Sciences. 2018; 112: 159–167.
24. Gastaldi L, Battaglia L, Peira E, Chirio D, Muntoni E, Solazzi I, Gallarate M, Dosio F. Solid lipid nanoparticles as vehicles of drugs to the brain: current state of the art. Eur J Pharm Biopharm. 2014; 87: 433-444.
25. Ganesan P, Narayanasamy D. Lipid nanoparticles: Different preparation techniques, characterization, hurdles, and strategies for the production of solid lipid nanoparticles and nanostructured lipid carriers for oral drug delivery. Sustainable Chemistry and Pharmacy. 2017; 6: 37-56.
26. Mehnert W, Mader K. Solid lipid nanoparticles: production, characterization and applications. Advanced Drug Delivery Reviews. 2012; 64: 83-101.

27. Muller, R.H., Mader, K., Gohla, S. 2000. “Solid lipid nanoparticles (SLN) for controlled drug delivey: a review of the state of the art”, Eur J Pharm Biopharm, 50, 161-177.
28. Sengel-Turk CT, Hascicek C. Design of lipid-polymer hybrid nanoparticles for therapy of BPH: Part I. Formulation optimization using a design of experiment. J. Drug Deliv. Sci. Technol. 2017; 39: 16-27.
29. Blasi P, Giovagnoli S, Schoubben A, Puglia C, Bonina F, Rossi C, Ricci M. Lipid nanoparticles for brain targeting I. Formulation optimization. Int. J. Pharm. 2011; 419: 287-295.
30. Kumar Das S, Yuvaraja K, Khanam J, Nanda A. Formulation development and statistical optimization of Ibuprofen-loaded polymethacrylate microspheres using response surface methodology. Chem. Eng. Res. Des. 2015; 96: 1-14.
31. Gu B, Burgess DJ. Prediction of dexamethasone release from PLGA microspheres prepared with polymer blends using a design of experiment approach. Int. J. Pharm. 2015; 495: 393-403.
32. Turk CTS, Oz UC, Serim M, Hascicek C. Formulation and optimization of nonionic surfactants emulsified nimesulide-loaded PLGA-based nanoparticles by design of experiments. AAPS PharmSciTech. 2014; 15: 161-176.
33. El-Gendy N, Pornputtapitak W, Berkland C. Nanoparticle agglomerates of fluticasone propionate in combination with albuterol sulfate as dry powder aerosols. Eur. J. Pharm. Sci. 2011; 44(4): 522–533.
34. Dai J, Ruan BH, Zhu Y, Liang X, Su F, Su W. Preparation of Nanosized Fluticasone Propionate Nasal Spray With Improved Stability and Uniformity. Chem. Ind. Chem. Eng. Q. 2015; 21(3): 457−464.
35. Amasya G, Badilli U, Aksu B, Tarimci N. Quality by design case study 1: Design of 5-fluorouracil loaded lipid nanoparticles by the W/O/W double emulsion — Solvent evaporation method. Eur. J. Pharm. Sci. 2016; 84: 92–102.

Table 1. Actual values and variable leves designed through 32 factorial design of FP-loaded SLNs.

Formulation codes	Actual values		Variable levels in coded form				
	X1	*X2*	*X1*	*X2*	$X1^2$	$X2^2$	*X1X2*
SLN1	1%	2	-1	-1	1	1	1
SLN2	1%	4	-1	0	1	0	0
SLN3	1%	8	-1	1	1	1	-1
SLN4	2%	2	0	-1	0	0	0
SLN5	2%	4	0	0	0	1	0
SLN6	2%	8	0	1	0	0	0
SLN7	4%	2	1	-1	1	1	-1
SLN8	4%	4	1	0	1	0	0
SLN9	4%	8	1	1	1	1	1

Table 2. The RSD% values obtained for the analytical validation parameters

	0.5 µg/ml	**4 µg/ml**	**10 µg/ml**
Accuracy (RSD%)	1.43	2.34	0.55
Repeatability (RSD%)	1.92	1.55	1.30
Intermediate precision (RSD%)	1.89	1.80	1.19

Table 3. Observed and predicted responses of FP-loaded SLNs.

Formul Code	Responses			
	Observed Values		Predicted Values	
	*Q*1±SD (%)	*Q*2±SD (nm)	*Q*1±SD (%)	*Q*2±SD (nm)
SLN1	52.02	352.9	43.51	334.3
SLN2	37.70	203.8	47.55	223.5
SLN3	33.31	130.9	31.97	112.7
SLN4	35.70	243.5	36.36	253.4
SLN5	38.11	190.7	34.68	196.8
SLN6	27.07	131.2	13.39	140.1
SLN7	71.32	177.1	79.17	172.5
SLN8	94.65	178.4	71.78	170.0
SLN9	29.74	171.6	44.76	167.5

Table 4. Results of model co-efficients estimated by MLR and the ANOVA of the fitted model for all responses.

Responses	Model co-efficients			Regression analysis of variance			
	Factor	Co-efficients	*P* value	*F*	*P* value	R^2	Adj R^2
Q1	Intercept	34.6844		3.87	0.0530	0.7345	0.5449
	*X*1	+12.1133	0.0638				
	*X*2	-11.4867	0.0755				
	$X1^2$	+24.9931	0.0179				
	$X2^2$	-9.81070	0.2662				
	X1X2	-5.71750	0.4248				
*Q*2	Intercept	+196.7462		57.71	< 0.0001	0.9506	0.9341
	*X*1	-26.7500	*0.0013*				
	*X*2	-56.6333	*< 0.0001*				
	X1X2	+54.1250	*< 0.0001*				

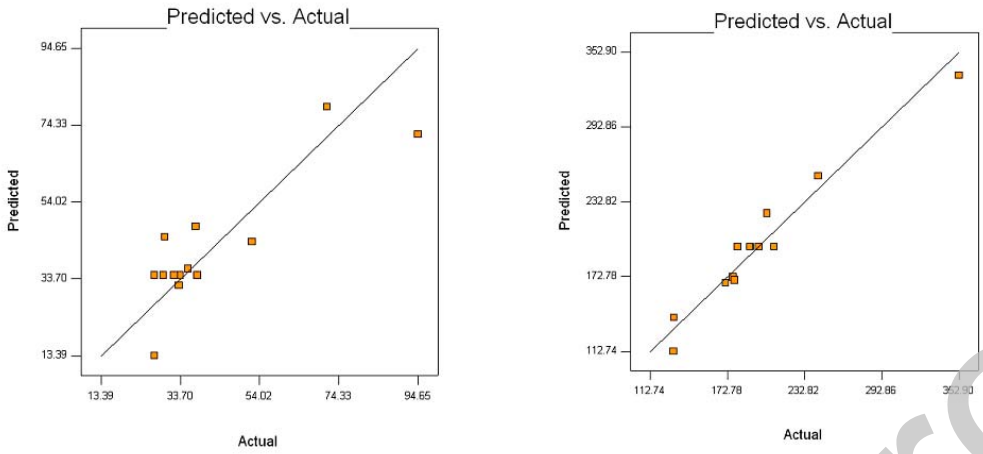

(A) (B)

Figure 1. Linearity correlation graphs between actual and predicted values of (A) *Q*1, (B) *Q*2.

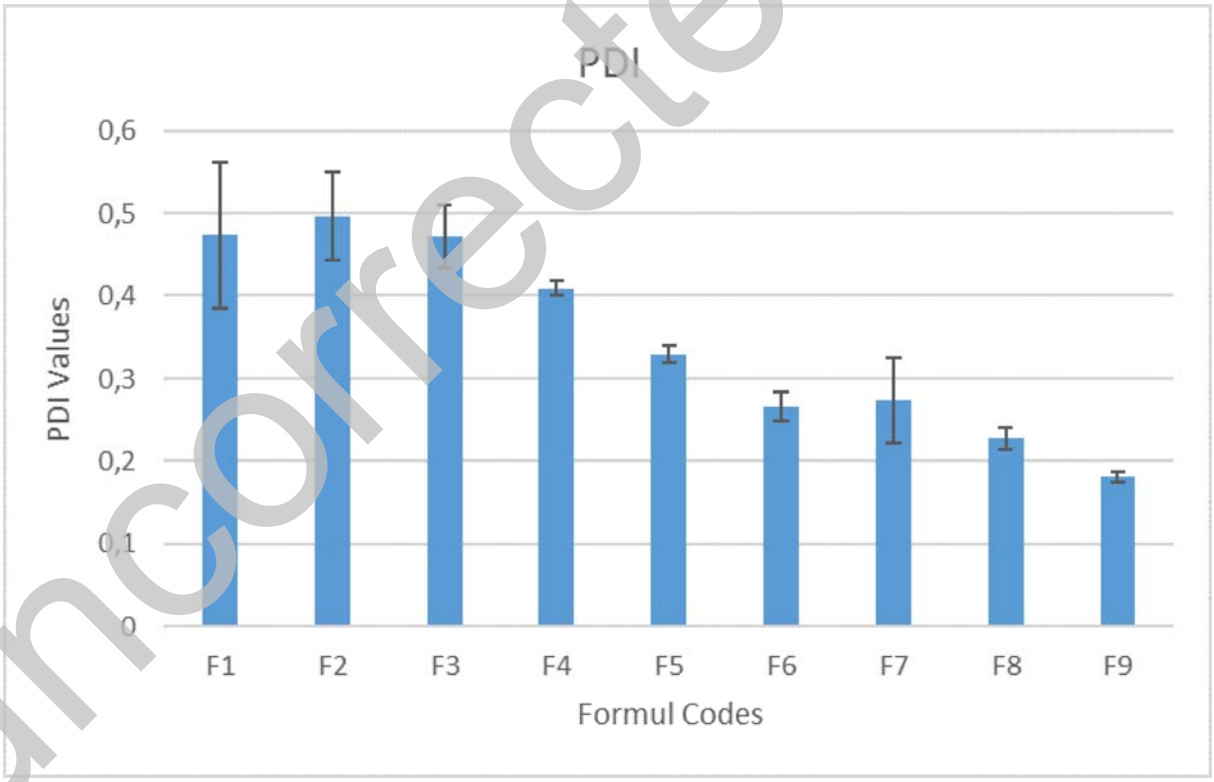

Figure 2. PDI values of the FP-loaded SLN formulations.

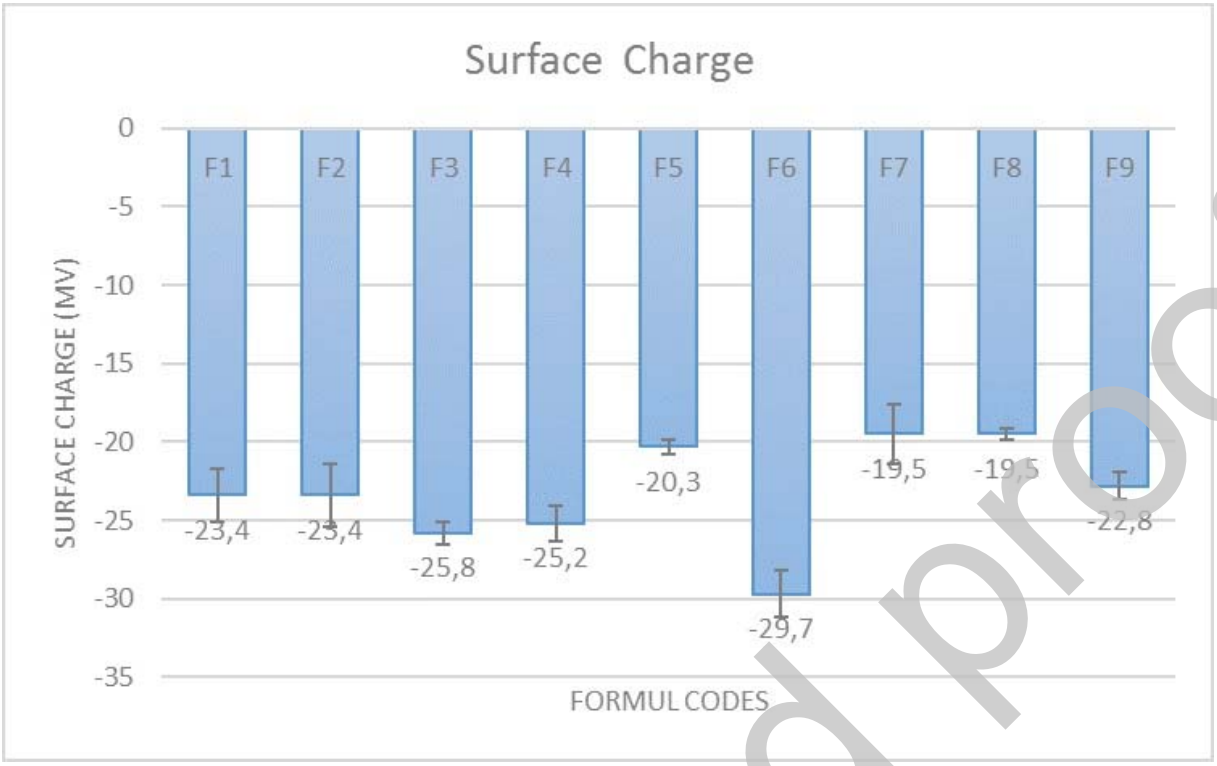

Figure 3. Surface charge of the FP-encapsulated SLN formulations.

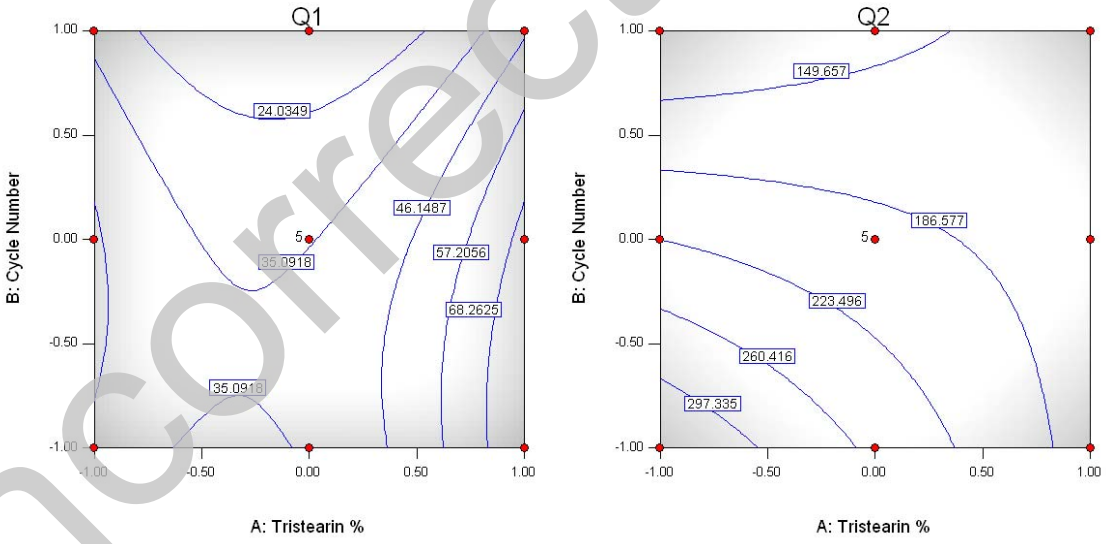

(A) (B)

Figure 4. Contour plots of FP-loaded SLNs showing the influence of X1 and X2 on (A) Q1, (B) Q2.

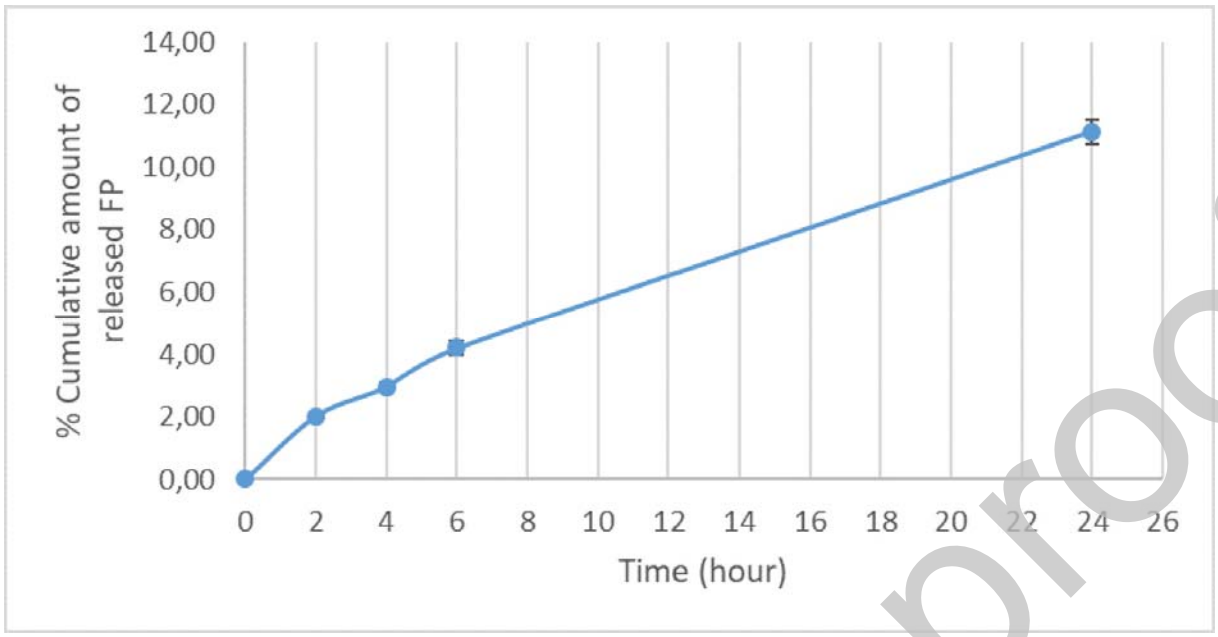

Figure 5. In vitro drug release profile of FP loaded SLN

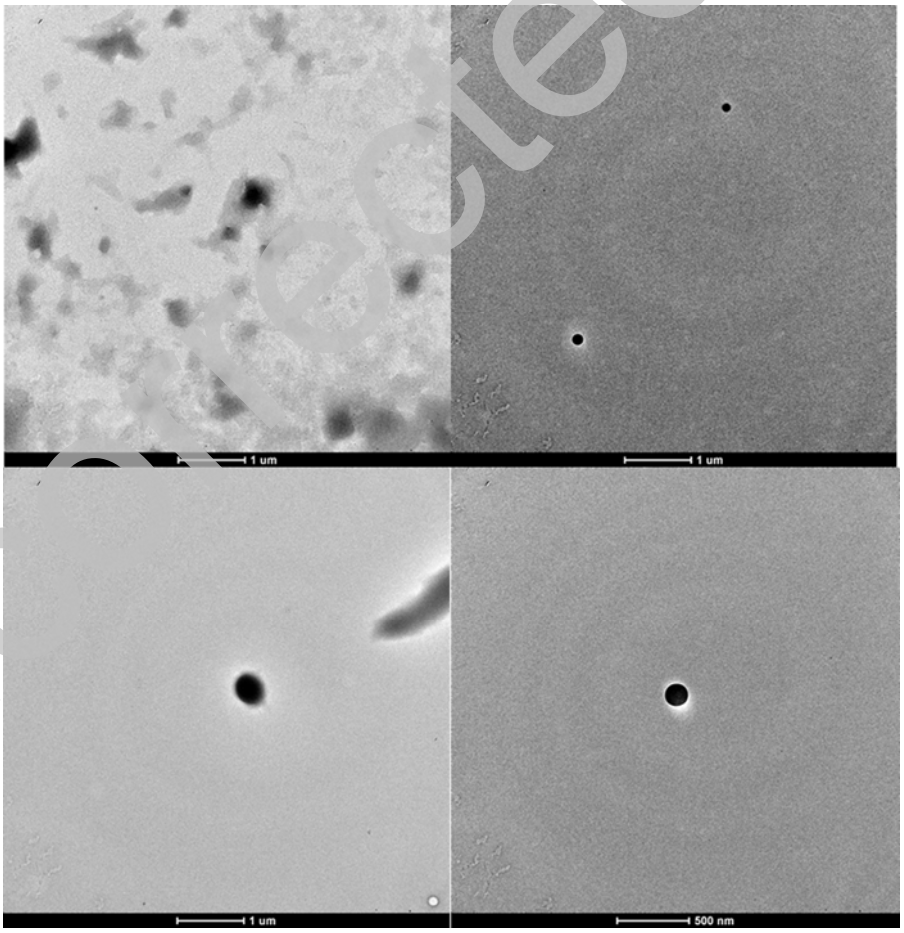

Figure 6. TEM micrograph of the optimal formulation

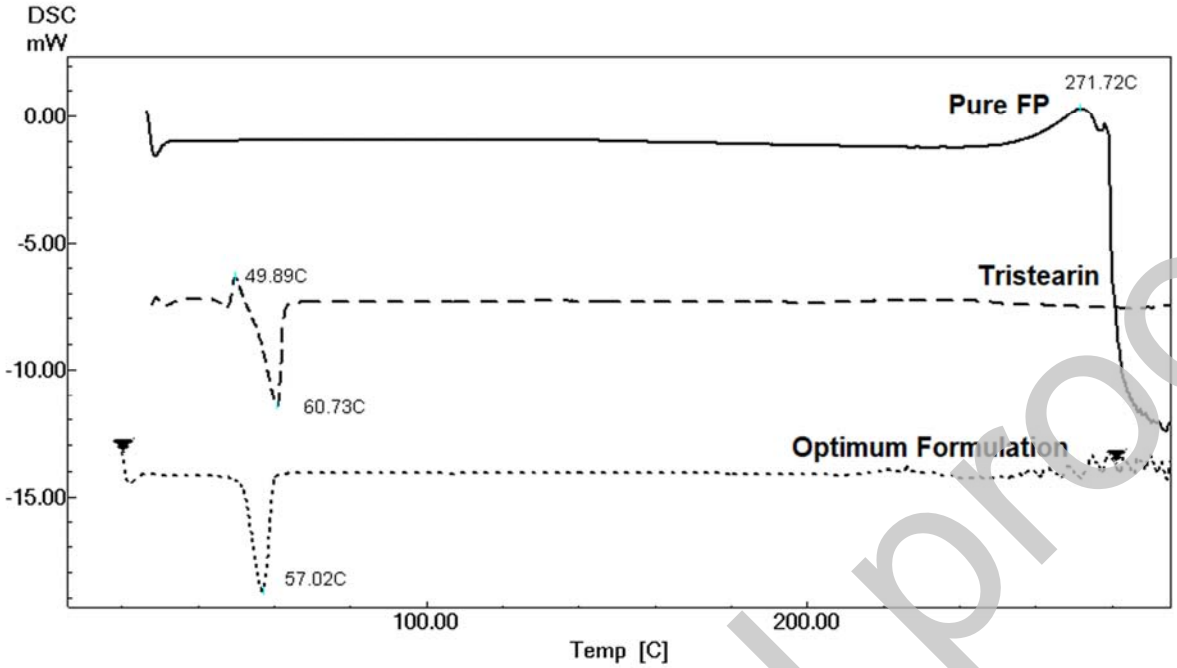

Figure 7. DSC thermograms of pure FP, Tristearin and optimum formulation.